Phase diagram for a driven vortex lattice in layered superconductors

I. Aranson
Department of Physics, Bar Ilan University, Ramat Gan 52900, Israel
and Argonne National Laboratory, 9700 South Cass Avenue, Argonne, Illinois 60439

A. Koshelev and V. Vinokur
Argonne National Laboratory, 9700 South Cass Avenue, Argonne, Illinois 60439
(Received 18 December 1996)

The dynamic phase transitions in a driven vortex lattice subject to quenched disorder are investigated by numerical simulations of the time-dependent Ginzburg-Landau-Lawrence-Doniach equations. We have considered a bilayered system as a prototype of multilayered current-carrying superconductors. Two transitions are examined: a dynamic melting transition, similar to single-layer systems, and a decoupling transition, which may occur only in a multilayered system. A universal structure of the phase-transition lines as functions of renormalized interlayer coupling and ''shaking temperature,'' which measures the disorder-induced effective Langevin force, is established. [S0163-1829(97)03134-2]

The properties of driven periodic structures (including charge-density waves, Wigner crystals, vortex lattices) subject to quenched disorder have become one of the central issues of the phenomenology of nonequilibrium statistical mechanics.[1–5] As it was proposed in Ref. 1 in the context of the vortex lattice, the driven system undergoes a dynamic phase transition at some threshold current between the fluidlike and crystallike moving states. The transformations of the moving states (dynamic phase transitions) were detected by anomalies in the I-V characteristics,[6,7] and by changes in correlation length[8–10] reflecting ordering of a moving lattice. To describe the transition, the concept of the ''shaking temperature'' $T_{\rm sh}\propto v^{-1}$, where v is the velocity of vortex motion, has been introduced. Shaking temperature measures the effective Langevin force exerted by the pinning centers on the moving vortices. Features of driven ordered state were found in Refs. 3,4, which revealed that even for large velocities the effect of static disorder persists and the lattice moves through elastically coupled highly correlated static channels. However most past numerical studies exploring the above ideas[1,4,5] were restricted to two-dimensional samples and to a range of small magnetic fields.

In this paper we investigate a bilayered system as a prototype of the multilayered superconductor. We examined two transitions: (i) dynamic melting, analogous to that in single layers, and (ii) dynamic decoupling where coherence in vortex motion in different layers breaks down upon lowering the driving force. We show the phenomenological description of the dynamic effects of disorder in terms of shaking temperature to work fairly well in the vicinity of the dynamic melting transition. We find a ''sharp'' dynamic melting transition as a function of applied current. We also find regimes of aligned and decoupled pancake motion. However, our simulations do not provide strong evidence in favor of sharp alignment transition. We demonstrate that the nonequilibrium phase diagram can be effectively described by only two variables: shaking temperature and rescaled interlayer coupling constant. Using the Ginzburg-Landau approach, we uncover a scaling relation in the parameter space for the dynamic melting transition in pure two-dimensional samples. We also obtain the explicit expression for the shaking temperature in terms of relevant parameters of the time-dependent Ginzburg-Landau equation (TDGLE).

We describe the dynamics by TDGLE for layered superconductors which in its dimensionless form reads

$$(\partial_t + iEx)\Psi_l = (\nabla - i\mathbf{A})^2\Psi_l + \zeta_l(x,y)\Psi_l + (1-|\Psi_l|^2)\Psi_l + \eta(\Psi_{l+1}+\Psi_{l-1}-2\Psi_l), \quad (1)$$

where Ψ_l is the (complex) order parameter in the layer l. The unit of length is the coherence length ξ, the unit of time is $t_0=\xi^2/D$, D is the diffusion constant, the magnetic field H is measured in units of the upper critical field H_{c2}, and the unit of the electric field E, generated by a moving vortex lattice, is $\hbar/2et_0\xi$. We choose the gauge $\mathbf{A}=(Hy,0,0)$ for the magnetic vector potential, where H is applied perpendicular to the surface of superconductor. We will assume a pure Josephson coupling between the layers characterized by the parameter $\eta=\xi^2/d^2\gamma^2$, where d is the interlayer spacing and γ is the anisotropy parameter. The pinning is described by a random function $\zeta_l(x,y)$ with the statistical properties

$$\langle\zeta_l(r)\rangle=0,\ \langle\zeta_l(r)\zeta_m(r')\rangle=\Delta\,\delta(r-r')\,\delta_{lm}, \quad (2)$$

where Δ is the pinning strength. The current within the layers is $\mathbf{j}_l=|\Psi_l|^2(\nabla\varphi_l-\mathbf{A})-\sigma E$. We consider the case of vanishing normal conductivity σ. In this limit the contribution from the normal current can be omitted and $E=$ const. The detailed numerical investigation of the current-carrying state in the presence of disorder is a serious computational challenge because even in reduced units the system is still controlled by four independent dimensionless parameters: E, H, Δ, and η. However, the study of the phase diagram can be significantly simplified: we will demonstrate soon the existence of universal scaling in the parameter space. This allows us to reduce the number of relevant parameters to

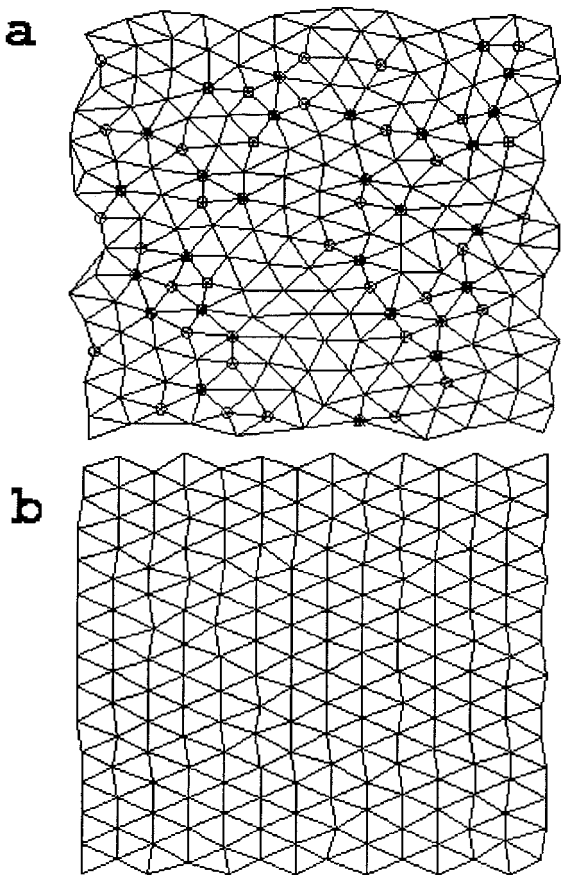

FIG. 1. Delauney triangulation of the vortex lattice. Direction of vortex motion is upwards. The parameters are: magnetic field $H=0.35$ the sample size $L_x\times L_y=$ 55.20×63.740 97, number of mesh points $N_x\times N_y=98\times 114$, the pinning strength $\Delta=$ 0.0005384. The number of vortices is 196. The transition occurs at $E\approx 0.002$. (a) Vortex configuration before the transition, $E=0.001$. The number of lattice defects is 70. (b) The defect-free vortex lattice after the transition, $E=0.004$.

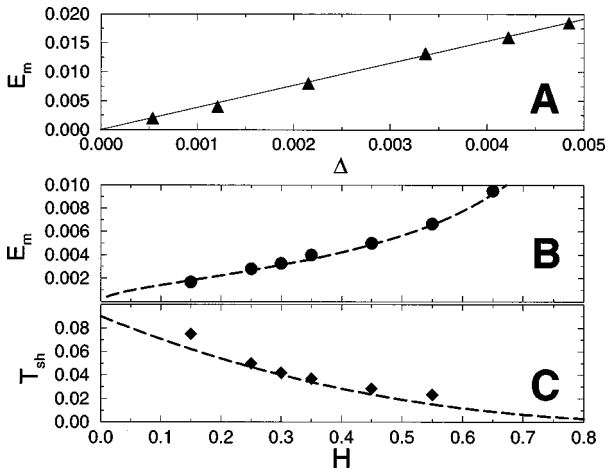

FIG. 2. E_m (triangles) as function of Δ at the transition point for $H=0.35$. (b) The electric field E_m as a function of magnetic field H for $\Delta=0.0012$. The symbols show numerical data, line shows the theoretic scaling relation $\sqrt{H}/(1-H)$. (c) The shaking temperature as a function of H. Symbols show numerical data, the line shows the melting temperature for clean two-dimensional samples.

only two: the shaking temperature, which is a combination of E, H, and Δ, and rescaled coupling, depending on η and H.

The explicit dependence on magnetic field can be scaled away in two limiting cases, $H\to 0$ and $H\to H_{c2}=1$. In the limit $H\to 0$, changing variables $\tilde{x}=\sqrt{H}x$, $\tilde{y}=\sqrt{H}y$, and $\tilde{t}=Ht$, reduces Eq. (1) to

$$(\partial_{\tilde{t}}+i\tilde{E}\tilde{x})\Psi_l=(\nabla-i\vec{x}_0\tilde{y})^2\Psi_l+\tilde{\zeta}\Psi+\mu(\Psi_{l+1}+\Psi_{l-1}-2\Psi_l)+\frac{1}{H}(1-|\Psi_l|^2)\Psi_l, \tag{3}$$

where $\tilde{E}=E/H^{3/2}$, $\mu=\eta/H$, and $\tilde{\zeta}=(1/H)\zeta(x/\sqrt{H},y/\sqrt{H})$. Note that for $H\to 0$ the amplitude of order parameter $|\Psi_l|\approx 1$ almost everywhere (except the vortex core), and, therefore, the last term in Eq. (3) can be neglected (this maps the TDGL to the frustrated XY model).[11] Then the explicit H dependence disappears and the number of controlling parameters reduces to three. The next parameter to be scaled away is the amplitude of the electric field $\tilde{E}$ which is proportional to the mean vortex velocity, $v=E/H$. By going into a comoving frame one can eliminate an *explicit* dependence on E (to first order in v): in a homogeneous system E would have vanished completely, whereas in the inhomogeneous system the random potential fluctuates in the moving frame with the typical time scale $\tau\propto 1/E$. The pinning force, thus, resembles the thermal Langevin force, and therefore the effect of pinning fluctuations with time can be conveniently described by the concept of shaking temperature. The shaking temperature measures the average magnitude of the effective pinning and can be estimated from comparison of the correlation function $\zeta\Psi$: $\chi=\langle\tilde{\zeta}\tilde{\zeta}'\Psi\Psi'\rangle$ with the true thermal fluctuations correlator.[12] Going in a comoving frame and assuming that at large times $\Psi(r-vt)$ and $\Psi(r-vt')$ are uncorrelated, one arrives at

$$\chi\approx\langle\tilde{\zeta}\tilde{\zeta}'\rangle\langle\Psi(r-vt)\Psi(r-vt')\rangle=2T_{\rm sh}\delta(r-r')\delta(t-t'), \tag{4}$$

where the shaking temperature is defined as $T_{\rm sh}=C_1\tilde{\Delta}/\tilde{v}$, C_1 is the universal (for this model) constant, which will be calculated numerically. Substituting $\tilde{\Delta}=\Delta/H$ and $\tilde{v}=\tilde{E}=E/H^{3/2}$, we obtain

$$T_{\rm sh}=C_1\sqrt{H}\Delta/E. \tag{5}$$

We see now that at small magnetic fields the dependence on the electric field is also scaled out and the system is described by only two relevant parameters: the reduced coupling $\mu=\eta/H$ and the shaking temperature $T_{\rm sh}$.

A separate scaling can be obtained in the case of $H\approx H_{c2}=1$ within the lowest Landau levels (LLL) approximation. The explicit dependence on magnetic field is eliminated by substitutions $\tilde{t}=(1-H)t$, $\tilde{\Psi}=\Psi/\sqrt{1-H}$. Then the rest of parameters are rescaled as follows: $\tilde{E}=E/(1-H)$, $\mu=\eta/(1-H)$, and $\tilde{\zeta}(x,y)=\zeta(x,y)/(1-H)$. For the shaking temperature we find

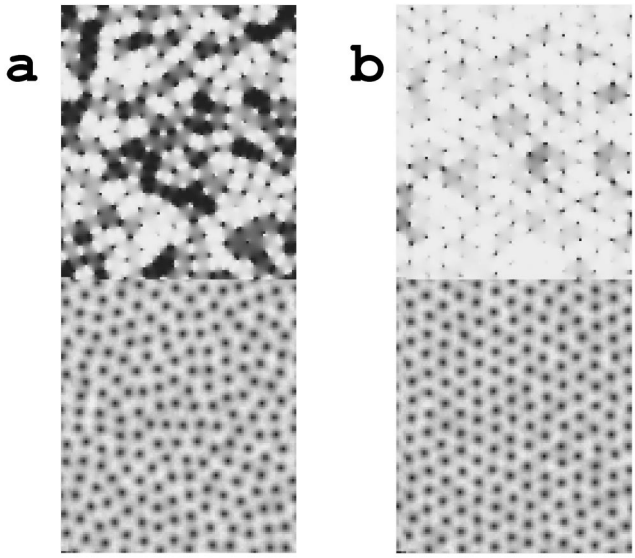

FIG. 3. Gray-coded images of $\cos(\phi_1-\phi_2)$ (top) and Ψ_1 (bottom). Dark and white shades correspond to min and max, respectively, $H=0.35, \eta=0.001$ and $\Delta=0.00215$. The number of vortices in each layer 196. For this set of parameters the alignment occurs at $E=0.0085$, and the melting at $E=0.0079$. (a) The decoupled vortex liquid for $E=0.0025$. The number of defects 80, $W_c=0.26$. (b) Aligned vortex crystal after the transitions, $E=0.01$, number of defects 6, $W_c=0.64$.

$$T_{\rm sh}=C_2\frac{\Delta}{(1-H)E}, \tag{6}$$

where C_2 is a constant. It is plausible to assume that the $H\to 0$ expansion matches the $H\to H_{c2}$ expansion at an intermediate region. That is possible only if $C_1=C_2=C_0$. Combining Eqs. (5) and (6), we obtain an interpolation formula for the entire range of the magnetic fields

$$T_{\rm sh}=C_0\frac{\sqrt{H}\Delta}{(1-H)E}, \quad \mu=\frac{\eta}{H(1-H)}. \tag{7}$$

One concludes from Eq. (7) that the phase diagram of the current-carrying superconductors is universal if plotted in the $\mu, \sqrt{H}\Delta/(1-H)E$ plane. Moreover, following the analogy between melting of the static vortex lattice in clean samples due to thermal fluctuations and the dynamic transition, we expect that $T_{\rm sh}$ at the transition point will coincide with the static melting temperature T_m. In the chosen scaling $T_{\rm sh}=T_m\approx 0.09$ for the two-dimensional (2D) case and for $H\ll 1$. This allows us to extract the constant C_0 from numerical simulations for two-dimensional samples.

To support the qualitative arguments we have studied TDGLE (1) numerically. We apply an implicit scheme (Crank-Nicholson) for a periodic system. The vector potential is introduced by link variables (see, e.g., Ref. 13). We study a system of 196 and 256 vortices per layer.[14]

We start with single layers. The crystallization transition line E_m is identified by an abrupt drop in the number of lattice defects which were located by Delauney triangulation applied to the set of vortex core coordinates. Shown in Fig. 1 is the change in the vortex configuration (a) before and (b) after the transition: note the total annihilation of defects in

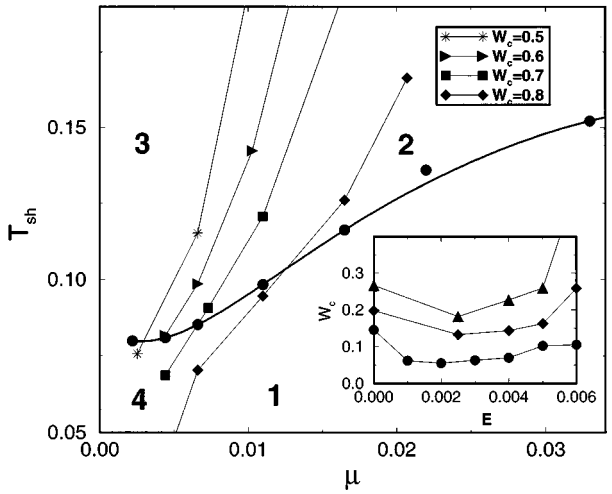

FIG. 4. (a) The phase diagram for bilayered system in $T_{\rm sh}-\mu$ plane, where $T_{\rm sh}=0.326[\sqrt{H}\Delta/(1-H)E]$, $\mu=\eta/H(1-H)$, for $H=0.35$ and $\Delta=0.00215$. The symbols show numerical data. The solid line depicts the ''dynamic melting transition,'' lines with symbols show contours of $W_c=$const. The numbers indicate four different states of the moving vortex lattice: 1 indicate the aligned vortex crystal, 2 indicates the aligned vortex liquid, 3 indicates the decoupled vortex liquid, 4 indicates the decoupled vortex crystal. Inset: W_c as function of E for $\eta=0.0005$ (circles), $\eta=0.001$ (diamonds), and $\eta=0.0015$ (triangles).

the ''crystalline'' high velocity phase. The shaking temperature is extracted from relation (4). Averaging χ over the entire sample and using that ζ is δ correlated, we end up with the following expression for the shaking temperature:

$$T_{\rm sh}=\frac{\Delta}{2S}\int_S d^2r\int_{-\infty}^{\infty}dt\langle\Psi(x,y,0)\Psi^*(x,y,t)\rangle, \tag{8}$$

where S denotes the area of the sample. The results of the simulations are comprised in Fig. 2. The dependence of the field E_m on the amplitude of pinning is shown in Fig. 2(a). The plot confirms the relation $E_m\sim\Delta$ predicted by the scaling relation (7). Shown in Fig. 2(b) is the dependence of E_m on the magnetic field for the fixed amplitude of pinning. Filled circles show the results of numerical simulations, the dashed line shows the best fit to the curve $\sqrt{H}/(1-H)$. As it follows from Fig. 2(b), Eq. (7) describes the behavior of $T_{\rm sh}$ over the whole range of the magnetic fields fairly well. The computations give the constant $C_0=0.326$.

In Fig. 2(c) we present the shaking temperature at the transition point measured according to Eq. (8) (diamonds) as a function of H. The dashed line shows the static melting temperature for vortex lattice in clean samples as a function of H: $T_m\approx 0.09(1-H)^2(1-0.3H)$.[15] This closeness of shaking temperature to the static melting line supports the entire concept of the shaking temperature and its relevance for the description of the dynamic phase transition.

Now we turn to layered systems. Since properties of the multilayers related to interlayer coupling can be captured by the simplest model of a two-layer superconductor, we restrict ourselves to the discussion of the phase diagram for bilayers. The most important effect expected to appear in multilayers is the alignment or entanglement (or decoupling) transition. As a measure of the coherent behavior of the vortices in

different layers we choose the phase-correlation functions $W_c=\langle\cos(\phi_1-\phi_2)\rangle$, where $\phi_{1,2}$ are the phases of the order parameter in layers 1 and 2, respectively. The gray-coded images of $\cos(\phi_1-\phi_2)$ and Ψ_1 for two different states are shown in Fig. 3. As we can see from Fig. 3(a), for small E vortices are not aligned, there exist extended regions with $\phi_1-\phi_2\approx\pi$. Thus, in the latter state vortices are effectively decoupled. Simulations show four apparently different dynamic states: aligned/misaligned crystals and aligned/misaligned liquids.

For strong coupling the liquid phase close to the melting point is strongly aligned. Further decrease of E leads to a smooth increase of the pancake misalignment. Our numerical simulations do not allow us to distinguish between the sharp alignment transition and smooth crossover. The transition, if it exists, must be continuous and can be found only by extensive size scaling analysis, which is beyond the scope of the present paper.

The phase diagram of bilayers in the $T_{\rm sh}-\mu$ plane is shown in Fig. 4. The position of the melting line and the contours of $W_c=$const, characterizing degree of alignment, are shown in the figure (in the perfectly aligned state $W_c=1$). We see that the melting temperature grows with the increase of η . For large η we reproduce the obvious result $T_{\rm sh}\rightarrow 2T_m$, where T_m correspond to the shaking temperature for a single layer.

A related comment is in order. First, we would like to draw attention to the behavior of the alignment parameter W_c as a function of vortex velocity $v\propto E/H$. We have found that W_c has a minimum at some value of the electric field, especially pronounced at small values of the coupling constant (see inset to Fig. 4). As we see, the degree of alignment first decreases with the increase of E, passes through the minimum, and then grows. The initial decrease of W_c shows that the Josephson coupling is suppressed for the slowly moving vortex lattice as compared to a static lattice. Such a suppression has been indeed observed experimentally. It was found that in the current-carrying Bean state (i) c-axis dissipation is enhanced[16,17] and (ii) the Josephson plasma frequency (proportional to $\sqrt{W_c}$) is reduced[18] as compared to static state obtained by field cooling.

In conclusion, we have examined the dynamic freezing (crystallization) and dynamic alignment, related to transitions from plastic to elastic dynamics of vortex configurations in three dimensions, and the four dynamic states: decoupled and aligned vortex liquids, and decoupled and aligned vortex crystals. A description of the combined effect of drive and disorder in terms of the shaking temperature leads to the dynamic phase diagram, isomorphic to the static diagram of the vortex state subject to thermal fluctuations.[19]

We are grateful to L. Krusin-Elbaum and T. Peterson for a critical reading of the manuscript. This work was supported by Argonne National Laboratory through the U.S. Department of Energy, BES-Material Sciences, under Contract No. W-31-109-ENG-38 and by the NSF-Office of Science and Technology Centers under Contract No. DMR91-20000 Science and Technology Center for Superconductivity.

[1] A. E. Koshelev and V. M. Vinokur, Phys. Rev. Lett. **73**, 3580 (1994).
[2] L. Balents and M. P. A. Fisher, Phys. Rev. Lett. **75**, 4270 (1995).
[3] T. Giamarchi and P. Le Doussal, Phys. Rev. Lett. **76**, 3408 (1996).
[4] K. Moon, R. T. Scalettar, and G. Zimányi, Phys. Rev. Lett. **77**, 2778 (1996).
[5] S. Ryu *et al.*, Phys. Rev. Lett. **77**, 5114 (1996).
[6] S. Bhattacharya and M. J. Higgins, Phys. Rev. Lett. **70**, 2617 (1993).
[7] M. C. Hellerqvist *et al.*, Phys. Rev. Lett. **76**, 4022 (1996).
[8] U. Yaron *et al.*, Phys. Rev. Lett. **73**, 2748 (1994).
[9] M. Marchevsky *et al.*, Phys. Rev. Lett. **75**, 2400 (1995).
[10] E. Rodriguez *et al.*, Phys. Rev. Lett. **71**, 3375 (1993).
[11] Y.-H. Li and S. Teitel, Phys. Rev. Lett. **66**, 3301 (1991); Phys. Rev. B **47**, 359 (1993); **49**, 4136 (1994).
[12] The thermal analogy holds only if (i) fluctuations in the velocity are small as compared to mean velocity and (ii) the $\chi(t)$ decays on the time scale which is the smallest one in the problem. The latter assumption breaks down, for example, for the moving perfect vortex lattice (Refs. 1 and 3).
[13] W. D. Gropp *et al.*, J. Comput. Phys. **123**, 254 (1996).
[14] In a periodic system the total number of vortices is defined by the applied magnetic field.
[15] This expression is a result of interpolation between the 2D melting temperature in the London regime $H\ll H_{c2}$ and in the vicinity of H_{c2}. See, e.g., M. Caillol *et al.*, J. Stat. Phys. **28**, 325 (1982); S. A. Hattel and J. M. Wheatley, Phys. Rev. B **50**, 16 590 (1995); M. Franz and S. Teitel, Phys. Rev. Lett. **75**, 521 (1995) ($H\ll H_{c2}$ melting); Z. Tešanović and L. Xing, *ibid.* **67**, 2729 (1991); Y. Kato and N. Nagaosa, Phys. Rev. B **47**, 2932 (1993); J. Hu and A. H. MacDonald, Phys. Rev. Lett. **71**, 432 (1993) (LLL melting).
[16] E. Rodriguez *et al.*, Physica B **194-196**, 2151 (1994).
[17] J. H. Cho *et al.*, Phys. Rev. B **50**, 6493 (1994).
[18] Y. Matsuda *et al.*, Phys. Rev. Lett. **78**, 1972 (1997).
[19] A. Koshelev (unpublished).